in Figure 10, the end-to-end distance of *cis*-PI in this system is close to the value in pure PI-13. Therefore, the smaller relaxation strength for *cis*-PI in the natural rubber network rather than that in the *cis*-PI network is due to the repulsive interactions between NR and *cis*-PI.

Conclusions

Due to relatively large experimental error involved and the limitation of the range of the sample molecular weight covered in this study, we cannot draw definite conclusions in the present stage. However, the following qualitative conclusions can be drawn:

1. The relaxation time τ_{ng} for the normal-mode process of the guest *cis*-polyisoprene in cross-linked natural rubber is longer than that in the undiluted *cis*-polyisoprene.
2. When M_x is lower than M_e, τ_{ng} becomes longer than that of the corresponding *cis*-PI. This result may be attributed to the strangulation effect.
3. The relaxation strength for the guest *cis*-PI in cross-linked natural rubber is smaller than that in pure *cis*-PI. This indicates that the mean-square end-to-end distance is smaller than the unperturbed dimension. However, $\Delta\epsilon$ for the guest *cis*-PI in the network prepared from a synthetic *cis*-PI sample is almost the same as the *cis*-PI in the bulk state.

Acknowledgment. B. T. Poh thanks the Japan Society of Promotion of Science for granting a fellowship to him to carry out this work. This work was supported in part by the Grant-in Aid for Scientific Research (60470107 and 6055062) by the Ministry of Education, Science and Culture, Japan. Support from the Institute of Polymer Research, Osaka University, is also acknowledged.

Registry No. Polyisoprene, 9003-31-0.

References and Notes

(1) Poh, B. T.; Adachi, K.; Kotaka, T. *Macromolecules*, second preceding paper in this issue.
(2) Poh, B. T.; Adachi, K.; Kotaka, T. *Macromolecules*, preceding paper in this issue.
(3) de Gennes, P.-G. *Macromolecules* **1986**, *19*, 1245.
(4) Ferry, J. D. *Viscoelastic Properties of Polymers*, 3rd ed.; Wiley: New York, 1980.
(5) Rouse, P. E. *J. Chem. Phys.* **1953**, *21*, 1272.
(6) de Gennes, P.-G. *J. Chem. Phys.* **1971**, *55*, 572.
(7) Doi, M.; Edwards, S. F. *J. Chem. Soc., Faraday Trans. 2* **1978**, *74*, 1789.
(8) See references cited in the preceding paper (part 2).
(9) Adachi, K.; Kotaka, T. *Macromolecules* **1984**, *17*, 120.
(10) Adachi, K.; Kotaka, T. *Macromolecules* **1985**, *18*, 466.
(11) Adachi, K.; Okazaki, H.; Kotaka, T. *Macromolecules* **1985**, *18*, 1687.
(12) Adachi, K.; Kotaka, T. *Macromolecules*, in press.
(13) Adachi, K.; Okazaki, H.; Kotaka, T. *Macromolecules* **1985**, *18*, 1486.
(14) Zimm, B. H. *J. Chem. Phys.* **1956**, *24*, 269.
(15) Shy, L. Y.; Eichinger, B. E. *Macromolecules* **1986**, *19*, 2787.
(16) Berry, G. C.; Fox, T. G. *Adv. Polym. Sci.* **1968**, *5*, 261.
(17) Adachi, K.; Kotaka, T. *Nihon Reoroji Gakkaishi* **1986**, *14*, 99.
(18) Vogel, H. *Z. Phys.* **1921**, *22*, 645.
(19) Klein, J. *Macromolecules* **1978**, *11*, 852.
(20) Nemoto, N.; Odani, H.; Kurata, M. *Macromolecules* **1972**, *5*, 531.

Transient Electric Birefringence Measurements of the Rotational and Internal Motions of a 1010 Base Pair DNA Fragment—Field Strength and Pulse Length Effects

Roger J. Lewis[†] and R. Pecora*

Department of Chemistry, Stanford University, Stanford, California 94305

Don Eden

Department of Chemistry, San Francisco State University, San Francisco, California 94132.
Received October 4, 1986

ABSTRACT: We examine the effects of the electric field strength and the orienting pulse duration on the measured decay of the transient electric birefringence of a blunt-ended DNA restriction fragment 1010 base pairs in length (molecular weight 670 000) in solution. Effects of pulse length on the distribution of decay times which were shown in an earlier work (Lewis, R. J.; Pecora, R.; Eden, D. *Macromolecules* **1986**, *19*, 134) are examined in greater detail, allowing us to determine the approximate time course for the excitation of each of the first three decay modes. The rise times of the first two modes are very similar, but the decay times are quite different. Two qualitative approaches are presented to explain the excitation time courses of the various modes. The first emphasizes the motion of different populations of counterions while the second postulates the exchange of excitation between different modes. In addition, by increasing the applied field strength, we observe a decrease in the average birefringence decay time before there is deviation from a modified form of the Kerr law. A similar decrease in the average decay time has been observed by Diekmann et al. (Diekmann, S.; Hillen, W.; Morgeneyer, B.; Wells, R. D.; Porschke, D. *Biophys. Chem.* **1982**, *15*, 263) and Stellwagen (Stellwagen, N. C. *Biopolymers* **1981**, *20*, 399).

Introduction

In previous work[1] we demonstrated that the zero-field electric birefringence decay from each of four monodisperse DNA fragments in solution could be resolved into several distinct exponential decays. We designated the slowest of these decay modes the "rotational decay mode" even though, in flexible DNAs, it probably represents a coupled bending-rotational motion. We attributed the faster decay modes to internal bending motions in the DNA fragments, although the possibility exists that these faster modes may contain a significant rotational component. The predictions of two dynamic models, the "trumbell" model of Roitman and Zimm[2-4] and the Rouse–Zimm model of Zimm,[5,6] compared favorably with the experimental results. The reader is referred to the earlier work[1,7] for additional details. Contrary to a statement in our earlier work[1] the

[†]Present address: Department of Emergency Medicine, Los Angeles County—Harbor—UCLA Medical Center, 1000 West Carson Street, Torrance, CA 90509.

0024-9297/87/2220-2579$01.50/0

Roitman–Zimm trumbell model does not include the effects of hydrodynamic interactions. Recent work by Nagasaka and Yamakawa includes hydrodynamic interactions in the trumbell model.[8]

The purpose of this work is to examine in greater detail the transient electric birefringence of a 1010 base pair (bp) DNA fragment (molecular weight 670 000).[9] We present data on the dependence of the birefringence decay modes on pulse width and field strength, as determined by DISCRETE[10,11] and CONTIN,[12-16] data analysis programs that are described in the earlier work[1] and below. The data allows us, after analysis by DISCRETE, to determine the approximate amplitude contributions of the first three decay modes to the birefringence decay, as a function of the length of the orienting pulse. It is important to note that in varying the pulse duration the field strength was not held constant, as it would have been impossible to do so and maintain an adequate signal-to-noise ratio across the entire span of pulse widths and at the same time minimize electrical heating of the sample. This complicates the interpretation of the data since, even at low field strengths, the distribution of decay times is slightly voltage dependent. Nonetheless, the semiquantitative data on the time dependence of the excitation of the modes shows some unexpected behavior. In addition, measurements of the effect of the electric field strength on the observed decay, with the pulse duration held constant, demonstrate that nonideal behavior is observed at field strengths below that at which deviation from a modified form of the Kerr law first occurs. (The Kerr law states that the steady-state birefringence is proportional to the square of the applied electric field.) In the discussion we qualitatively analyze the time course of the excitation of the various modes and the deviations that are observed from simple behavior, concluding that these deviations may be explained by postulating that the different dynamic modes, represented by the first two discrete decays, are able to exchange excitation energy with each other or by postulating that the motions of counterions occur on relatively long time scales and are coupled to the excitation of the modes.

A cornerstone of this and the earlier work[1] is the analysis of electric birefringence decay data by the programs CONTIN[12-16] and DISCRETE.[10,11] CONTIN finds the smoothest continuous distribution of decay times that is consistent with the data, given its precision. Thus, CONTIN is able to demonstrate the existence of distinct decay modes because it can distinguish a broad monomodal distribution of decay times from a bimodal or higher order distribution. All CONTIN results shown in this work have been fully smoothed (for a discussion of this point see ref 1 and 12–16). DISCRETE, on the other hand, assumes that the decay consists of a sum of discrete exponential decays. It finds the smallest number of such decays that are required to represent the data. Because of this, a broad monomodal distribution of decay times might be fit by DISCRETE as a sum of several exponentials, as more than one discrete exponential would be required to fit the data to its inherent precision. Thus it is important to fit data by using both programs to ensure that DISCRETE is not overestimating the number of distinct decay modes. When CONTIN and DISCRETE agree as to the number of decay modes, it is strong evidence that the data is adequately presented by a sum of distinct decaying exponentials. It is possible, however, that the distinct decays obtained by this method are themselves composites of exponential decays too closely spaced to be resolved.

Experimental Methods

The 1010 bp DNA fragment that was used in the following work was obtained as previously described.[9] After isolation and purification, the DNA fragment was ethanol precipitated and resuspended in 1 mM sodium phosphate buffer, pH 7.0 ($[Na^+]$ = 1.5 mM), at a concentration of approximately 10 μg/mL. This DNA solution was then dialyzed against several liters of 0.7 mM sodium phosphate buffer, pH 7.0 ($[Na^+]$ = 1.0 mM), at 4 °C overnight. Impedance measurements confirmed the final ionic strength of the DNA solution. The electric birefringence experiments and the data analyses were performed as before.[1] The field strengths ranged from 375 to 4400 V/cm and the data sampling interval ranged from 0.16 to 2 μs. All measurements were performed at 20 °C.

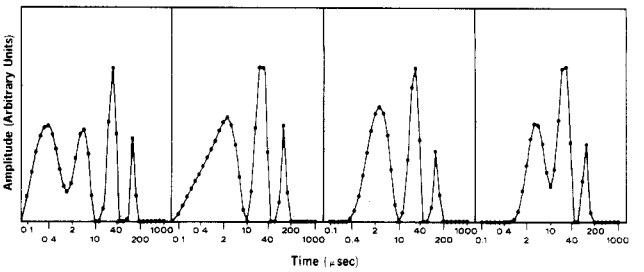

Figure 1. CONTIN analyses of birefringence data taken with a 0.64-μs sample time after a 128-μs orienting pulse of varying strength. The first panel shows the results after a 375 V/cm pulse, the second after 535 V/cm pulse, the third after a 790 V/cm pulse, and the last after a 1300 V/cm pulse. By simple inspection the results are independent of field strength. The changes observed in the form of the solution for decay times shorter than approximately 2 μs are probably not significant as the decay data was collected only every 0.64 μs.

Results

One of our basic goals is to understand the motions that a macromolecule undergoes in an unperturbed solution. An assumption in our use of transient electric birefringence in pursuit of this goal is that the motions produced by the relaxation from electrical orientation are the same as those produced by thermal excitation. If we use only low field strengths, for which this assumption is presumably true, then we would expect to see no dependence of the observed decay times on the field strength. Any deviation from this ideal behavior would suggest that we are distorting the form of the normal dynamical motions of the system with our perturbation.

In order to determine the dependence of the zero-field decay spectrum on the strength of the orienting field, without confounding variables, we measured the decay after pulses of field strength 375, 535, 790, and 1300 V/cm. All pulses were 128-μs duration, and data was sampled every 0.64 μs. The CONTIN analyses of these decays are shown in Figure 1. We observe that, over the field strength range measured, there are no significant changes in the positions or magnitudes of the decays that are seen. The changes observed at decay times less than approximately 2 μs are not significant because data was collected only every 0.64 μs. The position of the rotational peak at 150–200 μs and the first internal decay at 30–40 μs is consistent with our previous measurements. When CONTIN is used to analyze decays consisting of significant contributions from three or more decay times, the data are rarely accurate enough to precisely determine the time constants of each of the decays and we see an experiment to experiment variability in peak positions on the order of 30%. Taking this variability into account, the time constants we observe in this work are consistent with those we previously reported.[1] Note in Figure 1 that the relative size of the rotational peak and the first internal decay peak is essentially constant despite greater than a factor of 3 change in orienting field strength. This apparent uniformity is in marked contrast to the obvious changes in

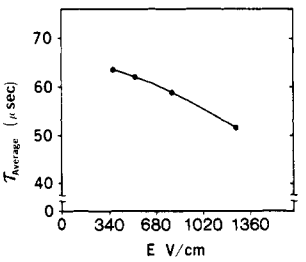

Figure 2. The solid circles show the average decay time of the data whose CONTIN analyses are shown in Figure 1. We see a definite decrease in the average decay time as the strength of the orienting pulse is increased. Even when the data at the two lowest field strengths are compared, this effect is significant, as the standard error in each of the points is approximately the radius of the plotted points.

the weights of the various decay modes seen when the pulse width is also varied, as shown below.

We can fit the data whose analyses are discussed above to a single exponential with a floated base line, in order to get a simple and reproducible measure of an "average" decay time. Diekmann et al.[17] have reported a similar method. The single exponential does not adequately represent the data, and thus the actual value that we obtain for this average decay time depends on the region of the decay over which we fit the data. In the work presented below we always fit between 640 and 900 sampling times starting at the beginning of the decay. When directly comparing average decay times obtained in this manner, we are careful to fit the data over exactly the same time interval. We have chosen this method for determining an "average" decay time because it allows the most direct comparison of our results with those of Diekmann et al.[17] For each case in which a comparison of these average decay times is made we have also compared the first moment of the distribution of decay times as determined by CONTIN, obtaining qualitatively identical results.

When we measure the average decay time, in the manner discussed above, and plot the results in Figure 2, it becomes evident that the average decay time decreases as the orienting field strength increases. Although it is not possible by eye to see the difference in the decay process in the analyses shown in Figure 1, CONTIN's numerical analysis of those results also show that the average decay time, as determined by the first moment of the distribution of decay times, decreases as the field strength is increased. It is not possible to determine with certainty from numerical analysis of the CONTIN solutions, because of the experiment to experiment variability already mentioned, whether the change in the average decay time is caused by a decrease in the decay time of one or more of the individual decay processes or whether the relative weights of the faster decay processes are increased by the stronger field.

Work by Stellwagen[18] and Diekmann et al.[17] has shown, in shorter DNA fragments and at higher field strengths than those used here, that the weights of the decay processes, but not their decay times, are influenced by field strength. In accord with our observations, the average decay time decreased as the orienting field strength was increased. The effect that Stellwagen[18] and Diekmann et al.[17] observed was much greater in magnitude than the effect that we have observed, presumably because of the relatively large field strengths used in their work. This allowed Diekmann et al.[17] to clearly show that the source of the decrease in the average decay time with increasing field strength was an increase in the relative magnitude of the first internal mode. Presumably this effect and the

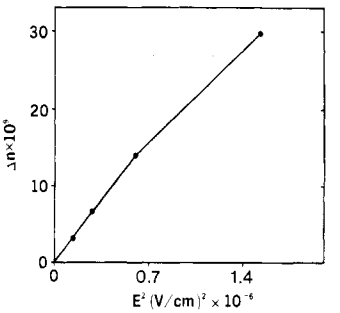

Figure 3. The observed birefringence after a 128-μs pulse as a function of the square of the applied field strength. By definition, a birefringent system obeys the Kerr law if the observed steady-state birefringence is proportional to the square of the applied field strength. We are using a defined pulse length but consider our modified Kerr law to be obeyed over the field strength range where the plot is linear. The four points correspond to the four field strengths shown in Figures 1 and 2. We see that the modified Kerr law is obeyed for the first three field strengths even though Figure 2 shows a field strength dependence of the average decay time in this region. The modified Kerr law is not obeyed at the highest field strength.

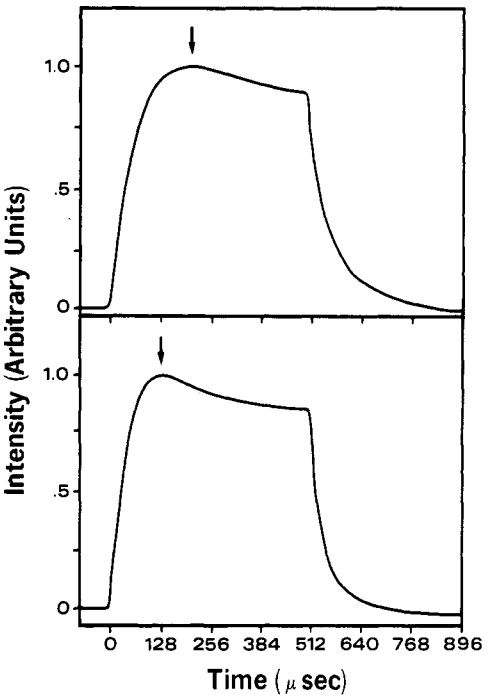

Figure 4. The observed birefringence, both during and after a pulse of 512 μs, for two different field strengths. The top panel shows the observed birefringence during and after a pulse of 375 V/cm. The arrow points to the maximum birefringence at approximately 200 μs after the start of the pulse. The bottom panel shows the observed birefringence during and after a pulse of 1300 V/cm. Again the arrow points to the maximum birefringence, but in this case it occurs at approximately 130 μs. The vertical scales are different for the two panels.

effect that we have observed are the same, allowing us to conclude that it is changes in the relative amplitudes of the decay modes and not their decay times that are responsible for the decrease in the average decay time with increasing field strength.

Commonly a comparison of the field strength dependence of the steady-state birefringence is compared with the Kerr law in order to determine whether a particular field strength is the low-field limit. Figure 3 shows a similar plot, with the four points corresponding to the four field strengths shown in Figure 2. Instead of steady-state birefringence we have plotted the birefringence at the end of a 128-μs pulse. Our reason for using this modified form

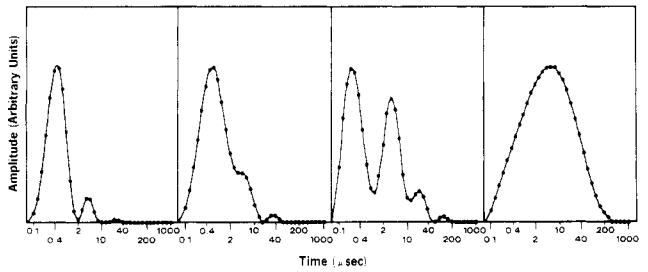

Figure 5. CONTIN analyses of zero-field transient electric birefringence decay data collected with a 0.16-μs sample time. The first panel shows the results after a 0.35-μs orienting pulse of 4400 V/cm. The second panel shows the results after 2.0-μs pulse of 1900 V/cm. The orienting pulse for the third panel was 8.0 μs in duration at 1300 V/cm, and for the fourth panel it was 32.0 μs in duration at 630 V/cm.

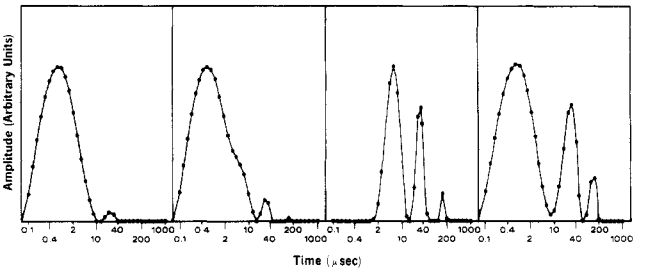

Figure 6. CONTIN analyses of birefringence data taken with a 2.0-μs sample time. The first panel shows the analysis of data after a 2.0-μs pulse of 1900 V/cm, the second after an 8.0-μs pulse of 1300 V/cm, the third after a 32-μs pulse of 630 V/cm, and the fourth after a 128-μs pulse of 375 V/cm.

of the Kerr law can best be understood by examining Figure 4. After a 512-μs pulse of either 375 (top panel) or 1300 V/cm (bottom panel) the birefringence has not reached a steady state, although it passes through a maximum at 125–200 μs depending on the orienting field strength. There does not exist, to our knowledge, a theory of birefringence, that could reasonably be expected to fit and account for these curves; nor is it clear, if we extended the pulse duration far beyond 512 μs, when in the curves the electrical orientation would stop and electrophoretic orientation or convective effects might begin. For these reasons we cannot measure a steady-state birefringence for strict comparison with the Kerr law. Instead we have chosen to use the value of the birefringence at 128 μs, a point before the maximum birefringence for a field strength of 375 V/cm and approximately at the maximum birefringence for a field strength of 1300 V/cm. We note below that for a simplified model of the excitation/orientation of a birefringent system with multiple decay times, we would predict that our modified Kerr law would be obeyed for an orientation pulse of arbitrary duration. In addition, we note that a deviation from our modified Kerr law caused by the shifting of the maximum of the birefringence toward 128 μs with increasing field strength would cause the high field strength points to be above the line set by the low field strength points. The usual deviation observed is that the high field strength points lie below the line set by the low field strength points.[18] The deviation that we observe in Figure 3 occurs only at the highest field strength where the point lies below the line set by the early points. It is clear from Figure 2, however, that changes in the average decay time are observed at a much lower field strength. Thus field strengths in the region where the modified Kerr law is obeyed do not ensure simple transient electric birefringence behavior.

In the earlier work[1] it was asserted that the length of the orienting pulse determined in large part the relative contributions of the different decay modes to the observed decay, with the longer orienting pulses exciting the slower decay modes to a greater extent relative to the faster decay modes. The data qualitatively supported that assertion. In order to better characterize this effect, we have measured the birefringence decay as a function of excitation pulse width, holding the sample collection time constant. As noted above, the orienting field strength was not held constant in order to maintain an adequate signal-to-noise ratio. This unfortunately convolutes the effects of pulse width with the effects of field strength shown above. In the discussion below we separate, to the extent possible, the effects of pulse width from those of field strength.

Figure 5 shows four CONTIN analyses of birefringence decays, taken after orienting pulses of width 0.35, 2.0, 8.0, and 32.0 μs, each measured with a data sampling time of 0.16 μs. Because the sampling time is fast relative to most of the decay times present, we are able to resolve the faster decay components most successfully. The shorter orientation pulse lengths excite the faster decays to a greater extent relative to the slower relaxation processes. Looking at the first panel we see three resolved decay processes. The fastest occurs with a characteristic time of approximately 0.4 μs, the next at about 3–4 μs, and the slowest at approximately 25–35 μs. The data collection time of 0.16 μs is only slightly faster than the 0.4-μs decay time of the fastest peak; therefore, the fastest peak may or may not be significant. As the orientation pulses become longer, as seen in the next two panels, we observe the distribution of decay times shift toward the slower times, but the positions of the peaks remain unchanged within the precision of the technique. By the third panel (8.0-μs orientation pulses) we see the detection of a decay process at 100–200 μs. This is the slowest decay process for this DNA and is presumably related primarily to rotation of the entire molecule.[1,18-20] When we use the longest orientation pulse (32.0 μs) and collect data on a 0.16-μs time scale, we are exciting the slower decay modes but collecting data over too short an interval to adequately characterize these slow decay processes. Because of this, CONTIN is unable to resolve the separate decay processes and finds the smoothest distribution of decay times that is consistent with the decay data obtained. This solution is shown in the fourth panel. To adequately characterize these slower decay processes, we must use an orientation pulse of sufficient duration and collect data over a longer period of time.

At this point it is useful to point out that the relative amplitudes of the various decays, as shown in the panels of Figures 5 and 6 below, vary both because of varying pulse width and because of varying orienting field strength. The left most panel corresponds to the highest orienting field strength and the shortest pulse length. Both a short pulse width and a high field strength selectively excites the faster decays over the rotational decay. Thus the changes we see in Figures 5 and 6 are the combination of two effects that we wish to separate, at least qualitatively. A determination of the average decay time performed on the data whose CONTIN analyses are shown in Figure 5 simply confirms that the longer pulses, at lower field strengths, excite the slower modes to a greater extent than the shorter pulses, at higher field strengths; i.e., we observe a lengthening of the average decay time with longer duration, lower field strength pulses. With a 0.35-μs 4400 V/cm pulse the average decay time is approximately 12 μs while after a 32-μs 630 V/cm orientation pulse it is over 50 μs.

In Figure 6 we see the CONTIN analyses of birefringence decays that have been measured with a 2.0-μs sampling

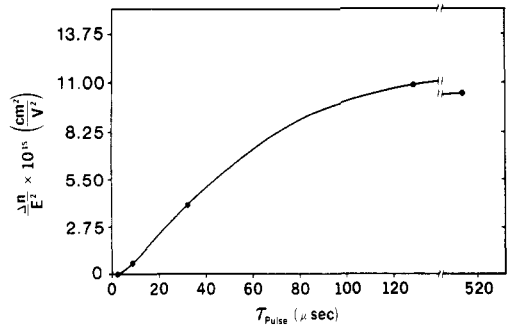

Figure 7. The time course of the excitation of the rotational decay mode is shown in this figure. The fraction of the total birefringence associated with the rotational decay mode has been normalized by the square of the applied field strength and plotted as a function of pulse duration. See text for discussion.

time. This longer sampling interval, compared with 0.16 μs, allows us to obtain more information on the slower decay modes. The first panel in Figure 6 shows the CONTIN analysis of the birefringence decay after a 2.0-μs orienting pulse, the same length pulse as used in the second panel of Figure 5. Because of the slower sample time, CONTIN is not able to resolve the processes previously seen at 0.4 and 3–4 μs and we obtain a single broad peak over the entire region. The program is able, however, to resolve the decay at 25–35 μs. Again we see that as the length of the orientation pulse is increased from 2.0 to 8.0 μs, then to 32 μs, and finally to 128 μs in the last panel, the slower decays are excited to a larger and larger extent. The orienting field strength was 1900, 1300, 630, and 375 V/cm for the four panels, respectively. The variability in the solutions that we see on time scales faster than approximately 5 μs is not significant given the data collection interval of 2 μs.

We can fit the data to a single exponential, as described above, in order to quantify the changes seen in Figure 6. For pulse lengths of 2.0–128 μs, with the field strength changes noted above, we find the average decay time increases as the length of the orientation pulse increases. With a 2.0-μs 1900 V/cm pulse the average decay time is approximately 25 μs, while with a 128-μs 375 V/cm pulse the average decay time is approximately 80 μs. This average decay time of 80 μs after 128-μs 375 V/cm pulse should not be compared with the average decay times shown in Figure 2 because of the different sampling intervals used. However, when we increase the orientation pulse width from 128 to 512 μs, holding the field strength constant at 375 V/cm, the average decay time *decreases* to about 75 μs. This unexpected decrease will be discussed below.

A visual comparison of Figures 1 and 6 shows that the effects of varying pulse width on the distribution of decay times is much greater than the effects of varying the field strength, over the range of pulse durations and strengths tested. This allows us to temporarily neglect the effects of field strength for purposes of the qualitative discussion that follows.

Using DISCRETE to resolve the various decay modes from each other and from a knowledge of the total absolute birefringence observed in the solution, we have calculated the birefringence amplitude associated with each decay mode for the data shown in Figures 5 and 6. In order to maintain adequate signal to noise ratios over a wide range of pulse widths, it was necessary to vary the orienting field strength. Since the orienting field strength affects the zero-field decay, as observed above, we are precluded from an accurate quantitative interpretation of these data on the time course of the excitation of the various decay modes.

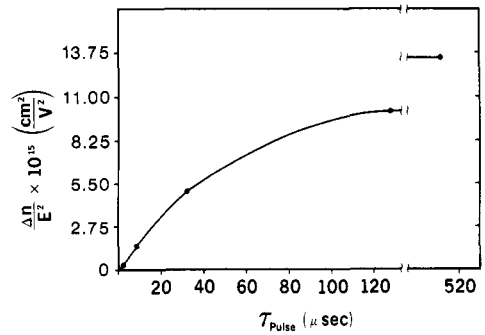

Figure 8. The excitation of the first internal mode as a function of pulse length is shown in this figure in an analogous manner to the presentation in Figure 7. We see a significant increase in the amplitude of this decay mode from 128 to 512 μs.

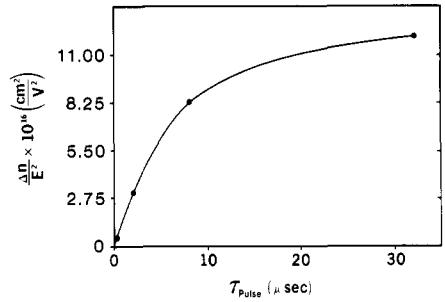

Figure 9. The time course of excitation of the second internal decay mode. The method of presentation is the same as that of Figures 7 and 8.

Figure 7 shows the amplitude of the rotational decay (normalized by the square of the orienting field strength) as a function of the orienting pulse width. Unlike the curve for a simple excitation process, which would have the greatest slope at the start of the pulse, the excitation of the rotational mode shows a "lag" for at least 2 μs. By 128 μs the rotational mode is essentially fully excited as there is no significant change in its amplitude between 128 and 512 μs. The rotational mode decays with a characteristic time around 170 μs.[1] Thus it is excited more rapidly than it decays, under our experimental conditions.

Figure 8 shows the excitation of the first internal mode as a function of the duration of the orienting pulse. In contrast to the rotational mode, this mode is excited without a discernible lag and the amplitude of the first internal mode shows a significant increase between 128 and 512 μs. This accounts for the observed decrease in the average decay time when the duration of the orienting pulse is changed from 128 to 512 μs. For comparison, the decay time of the first internal mode is approximately 37 μs.[1]

We note here that the excitation time scales and birefringence amplitudes of the rotational and first internal modes are quite similar.

Figure 9 shows the excitation of the second internal decay mode. This mode is excited without any observed lag and up to the observed pulse width of 32 μs no unusual behavior is seen.

The large field strengths used in experiments with pulse lengths of 0.35 or 2.0 μs may make the early points of Figures 7–9 less accurate than the later points. This is because the birefringence data have been normalized by E^2 in a field strength region where there is a slight deviation from our modified Kerr law.

Discussion

In order to clearly discuss the pertinent deviations from simple excitatory behavior that we have observed in the

decay modes of this DNA fragment, we begin by describing what we consider "ideal" behavior. Ideal behavior will be used here to refer to the low-field limit of the dynamics calculated by Benoit[21] for a rigid rod oriented by an anisotropic electrical polarizability oriented along its long axis. In this case, including amplitude terms to E^4, the rise of the electric birefringence is of the form

$$\Delta n(t) \propto E^2(1 + kE^2)(1 - \exp(-6(1 - kE^2)\theta_r t)) \quad (1)$$

where the electric field of strength E is turned on at $t = 0$, k is a constant, and θ_r is the rotational diffusion constant. In the low-field limit the rise of the birefringence reduces to

$$\Delta n(t) \propto E^2(1 - \exp(-6\theta_r t)) \quad (2)$$

We see that in this simple case it is only in the low-field limit that the Kerr law is obeyed and the rise time is independent of field strength. The decay of the birefringence is predicted to be

$$\Delta n(t) = \Delta n_0 \exp(-6\theta_r(t - t_0)) \quad (3)$$

regardless of the orienting field strength or duration, where Δn_0 is the birefringence at $t = t_0$, when the field is turned off.

Unlike a rigid rod, a flexible DNA exhibits many decay processes which we examine separately. For each of the separate decay modes we consider ideal behavior to consist of [1] excitation according to eq 2 where $6\theta_r$ is replaced by a field-independent constant for the particular mode and [2] decay of the form of eq 3 where $6\theta_r$ is replaced by the same constant. We note that in this idealized situation each mode would separately satisfy the Kerr law after an orienting pulse of arbitrary duration; i.e., our modified Kerr law would be obeyed. Stellwagen[18] has observed that DNA, when short and monodisperse, exhibits the simple behavior predicted by eq 2 and 3 at low-field strengths. Mandelkern et al.,[22] on the other hand, have noted rise times approximately 5% greater than decay times for small DNA fragments.

An examination of Figures 7 and 8 shows that the excitation curves are qualitatively inconsistent with eq 2. In Figure 7 we note that the rotational mode is excited only after a lag of at least 2 μs. In Figure 8 we note a significant increase in the amplitude of the first internal mode from 128 to 512 μs even though both data sets were taken with the same orienting field strength. The excitation of the second internal mode shown in Figure 9 is qualitatively consistent with eq 2. By using the program DISCRETE to analyze the birefringence decay data, we have assumed that the decay consists of a sum of decaying exponentials. In other words, we have assumed that the decay of each mode is consistent with eq 3, but we have not assumed that the decay constants are field strength independent. The agreement between CONTIN and DISCRETE as to the number of decay modes in the data confirms the assumption of distinct exponentials.

We have shown here that the birefringence decay of flexible DNA is dependent on the orienting field strength. In general, one could imagine the relative amplitudes of the various decay modes and/or their decay times to be field strength dependent. As mentioned in the results, Diekmann et al.[17] and Stellwagen[18] have both shown that it is the relative amplitude of the decay modes and not the decay times that are field strength dependent. In addition we have shown here and previously[1] that is is the relative amplitudes of the decay modes and not their decay times that are pulse-width dependent.

The relative amplitudes of the various decay modes would be pulse-width dependent if they were each excited according to eq 2 but with different characteristic rise times. In addition we see that the average decay time would increase as the length of the orienting pulse is increased as the slower orienting (and presumably slower decaying) modes would have more time to reach their limiting amplitude. This is the behavior that we see, with one exception. We have noted that increasing the pulse length from 128 to 512 μs decreases the average decay time, even while holding the field strength constant. By resolving the rotational and first internal modes from the other modes and plotting their excitation (Figures 7 and 8), we see that the magnitude of the rotational decay is not significantly affected by increasing the pulse length from 128 to 512 μs but that the magnitude of the first internal mode is significantly increased. Since the first internal mode decays with a characteristic time around 30–40 μs but does not reach steady state by 128 μs, we believe that some process slows its excitation. Possibilities for this process include slow movement of tightly bound counterions or the transfer of excitation energy to the slowly exciting rotational mode. These ideas are considered below.

The excitation of the rotational mode shows some nonideal behavior as well. At early times (around 2 μs) we see a lag in the excitation of this mode (Figure 7). This could be explained by postulating that the polarization of the counterion atmosphere along the DNA requires a significant time period (on the order of 1–3 μs). Gebhard et al.[23] have measured ionic polarization times around 0.1–0.2 μs in shorter DNA fragments using field reversal birefringence. Porschke[24,25] has seen a delay in the orientation of short rodlike DNA fragments that is qualitatively similar but much shorter than the delay we see in the excitation of the rotational mode. The sample collection times used in our experiments are far too long to allow us to detect the lag seen by Porschke, if it occurs on the same time scale in our experimental system. It seems likely, however, that this putative polarization time has a strong contour length dependence and that we are observing the same process as Porschke. This possibility is also discussed in greater detail below. It is also possible that exchange of excitation energy between the various dynamic modes accounts for the lag in the excitation of the rotational decay mode. In a scheme below, we will assume that some of the energy in the first internal mode is transferred to the rotational mode. This could account for both the lag in the excitation of the rotational mode and the continued growth of the first internal mode between 128 and 512 μs.

A significant number of workers have studied the behavior of DNAs at various lengths and field strengths, examining either the steady-state birefringence[18,26–29] or the shape of the birefringence rise curve.[18,22,24,30] Suggested mechanisms for the behaviors seen have generally centered on a polarization of the counterion atmosphere.[24–36] It has been suggested that counterion polarization may be easily saturated[18,24,29,30,37,38] or may have a significant time constant.[22,24–26,32,39] The field strength and pulse length dependencies that we have observed in the decay of the electric birefringence suggest even more complex behavior in the case of flexible DNAs.

The birefringence rise curves provide evidence for complexity in the orientation mechanism. We see in Figure 4 that the birefringence curve goes through a maximum (shown by arrows) and then approaches a slightly smaller value. The time required to reach the maximum birefringence is decreased when the orienting field strength is increased (second panel). Interestingly, the progression from the maximum birefringence to a relatively steady

state occurs during the period from 128 to 512 μs, the same period during which the first internal mode continues to increase in amplitude while the magnitude of the rotational mode remains essentially constant. Other modes must be decreasing in amplitude for the total birefringence to decrease. One possible interpretation is that some process that occurs slowly between 128 and 512 μs is responsible for a selective increase in excitation of the first internal mode. If the decrease in the time required to reach the maximum birefringence with increasing field strength signifies an acceleration and/or accentuation of this slow process, then this would explain the decrease in the average decay time with increasing field strength that we have observed with a 128-μs orienting pulse (Figure 2). Likewise it would also explain the increase in the magnitude of the first internal mode that Stellwagen[18] and Diekmann et al.[17] observed with increasing field strength.

We note that a rigid molecule oriented by both an anisotropic polarizability and a permanent dipole moment can show rise curves not unlike that of our DNA.[40] We believe that the symmetry in DNA makes the occurrence of a significant permanent dipole moment unlikely, in agreement with others.[27,29,38] We should mention, however, that work by Stellwagen has suggested that in one small DNA fragment orientational properties similar to those of a permanent dipole appear to exist.[41]

We will now present two approaches to explaining the observations we have made. The first emphasizes the motion of different populations of counterions while the second emphasizes the postulated exchange of excitation energy between different dynamic modes.

In the first approach we wish to explain a fast polarization (DNA probably does not contain a permanent dipole moment and some orientation occurs after a pulse as short as 350 ns) and a slow polarization/orientation (the poorly defined process that occurs between 128 and 512 μs) by assuming that the majority of the polarization and orientation of DNA is directly related to motion of the counterions. To do so we postulate two different populations of counterions that are polarized with different characteristic times. We assume as well that the polarization of these two populations may interact and, in general, have different field strength dependencies. Rau and Charney[28,31] have attempted, with reasonable success at low ionic strength, to separate the electric polarizability of short DNA fragments into a contribution from the polarization from a Debye–Hückel counterion atmosphere and a contribution from the polarization of presumably condensed counterions.[42-44] These two populations, the condensed and loosely bound counterions, provide an intuitively appealing explanation for the existence of two different characteristic polarization times. We note that when one postulates two populations of any chemical species one must also consider the possibility that the two populations will exchange, further complicating the observed behavior (for an example, see ref 45).

Morita and Watanabe, who have worked extensively in this area,[46-48] have calculated the dynamics of counterions bound to a rodlike counterion subject to various potential functions.[32] Two cases, the free motion of counterions and the motions of counterions subject to an oscillatory potential, are of particular interest. In the first case their model predicts a single relaxation time, which is approximately proportional to the square of the rod length. In the second case two relaxation times are predicted, a fast time that corresponds to the restricted motion of the bound counterions in the individual potential wells and a longer time that corresponds to the time it takes the bound counterions to escape many different potential wells and thus redistribute themselves along the rod. It is easy to see that this second slower time will be highly dependent on the depth of the potential wells, the temperature, and the field strength. The discrete nature of the negative charge on DNA at the sites of the phosphodiester bonds provides a good a priori reason to suppose that the potential felt by condensed counterions would be periodic in nature. Thus we believe that the Morita and Watanabe work,[32] if we postulate that the potential wells are deep relative to the thermal energy, provides a simple explanation for a slow polarization/relaxation time for the movement of the subpopulation of counterions that are condensed.

What about the polarization of the loosely bound counterions? Porschke[24,25] interpreted his observations of a lag in the rotational orientation as suggesting that the characteristic polarization time is on the order of 10 ns for DNAs of 76 and 95 bp in length. Although Porschke attempted to determine the chain length dependence of this time by analyzing data from DNAs of 27 and 187 bp length, by his own assessment his data were inconclusive.[24] The model of Morita and Watanabe[32] (and others) predict a length-squared dependence for the relaxation time of freely diffusing loosely bound counterions and our DNA is between 10.6 and 13.3 times as long as Porschke's fragments. Thus the Morita and Watanabe theory would suggest that the relaxation/polarization of the loosely bound counterions would occur on our DNA at a time scale 100–200 times longer than on Porschke's DNA. As his lag in the orientation suggested a polarization time of 10 ns, this simple analysis would suggest that our lag would correspond to a polarization time of 1–2 μs. Give that we have completely ignored the flexibility in our longer DNA, this prediction is surprisingly close to the behavior that we see (Figure 7). Thus it is plausible that the lag in the excitation of the rotational mode is related to the polarization of loosely bound counterions and that this is the same lag that Porschke observed in much smaller DNAs.

This explanation of the lag in the excitation of the rotational mode may also explain the lack of such a lag in the excitation of the first and second internal modes. We envision the characteristic wavelength of the first and second internal modes as being substantially shorter than the contour length of the DNA. We expect the time it takes the loosely bound counterions to polarize along these shorter distances to be too short to be observed by our experiments because of the postulated length-squared dependence of the polarization time.

What could be the cause of the decrease in the observed birefringence between 128 and 512 μs (Figure 4)? Suppose, as suggested above, that the loosely bound counterions polarize with a time constant on the order of 1–2 μs but that the condensed counterions require on the order of 100 μs to polarize because of the depth of the periodic potential wells. In addition we recall that several workers[18,29,30,38] have found that their birefringence or dichroism results are consistent with an easily saturated polarizability and that the suggestion has been made[24,27] that at sufficient field strengths the loosely bound counterions are able to escape from the end of the macromolecules. These suppositions and published observations may be combined into a scheme that qualitatively accounts for many of our observations. The first step in the polarization of the DNA would consist of the polarization of the loosely bound counterions[31] and would be nearly complete after approximately 1 or 2 μs. This would be followed by the relatively slow polarization of the condensed counterions.

As the positive counterions are concentrated at one end of the DNA molecule, they would cancel an increasing fraction of the DNA's negative charge, allowing some of the loosely bound counterions to escape into the general solution. It has been calculated[31] and suggested[49] that the polarizability of loosely bound counterions is proportional to the square of the linear charge density. We would expect that a decrease in the effective charge density near one end of the DNA would decrease the polarizability of the counterions loosely bound to that section of the molecule. Thus the slow polarization of the condensed counterions would be closely followed by a decrease in the induced dipole moment of the highly polarizable loosely bound counterion field. This could account for the slight loss of orientation and birefringence that we see occurring between 128 and 512 μs. The fact that the slow polarization time of the condensed counterions in the periodic potential would be voltage dependent could account for the voltage dependence of the time to achieve maximum birefringence as seen in Figure 4.

There are several weaknesses in this model. For example, one would expect the sections of the DNA that are depleted of condensed counterions, because of their higher effective charge density, to have an increased polarizability and orientation. This might cancel the loss of polarizability and orientation occurring at other sections of the molecule, leaving us with no observed effect from the slow polarization of the condensed counterions. As a further complication we note that processes other than the polarization of different populations of counterions could result in multiple apparent polarization/orientation times. As an example, Fixman[50,51] has calculated the convective polarization of the counterions produced by the electrophoretic translational motion of the charged polyelectrolyte. One can easily see that convective effects of this sort could couple the polarization and dynamics of a flexible macromolecule in a complicated manner. In addition, we note that in general we would expect the different populations of counterions to interact, further complicating their dynamics. As a final caution we note that, at sufficiently high-field strengths, a field-induced reaction occurs in DNA.[52,53] We believe our field strengths were far below those required to cause such reactions, however.

One can also explain many of the behaviors that we have observed by constructing a "chemical kinetics" model, in which the different dynamic modes may be coupled, allowing them to exchange excitation energy. In this second approach we represent the amplitude or energy of each of the dynamic modes using the notation for the concentration of a chemical species. The chemical species "A" is the chain in thermal equilibrium. B_1 represents the chain with the rotational mode excited; i.e., the entire chain has been rotated by the orienting electric field. B_2 represents the chain with the first internal mode excited, and B_3 represents the chain with the second internal mode excited. The ideal behavior defined by eq 2 and 3 can be represented in this kinetics scheme by

$$\begin{aligned} [A] &\underset{k_{1r}}{\overset{k_{1f}}{\rightleftharpoons}} [B_1] \\ [A] &\underset{k_{2r}}{\overset{k_{2f}}{\rightleftharpoons}} [B_2] \\ [A] &\underset{k_{3r}}{\overset{k_{3f}}{\rightleftharpoons}} [B_3] \end{aligned} \tag{4}$$

In the absence of an electric field the forward rate constants are zero and the solution consists of only species A (neglecting thermal fuctuations). The zero-field values of each of the reverse rate constants are the inverses of the decay times of the respective modes. The application of an external electric field results in nonzero forward rate constants and the subsequent buildup of a small but significant amplitude of each of the birefringence modes. During this buildup period, if only eq 4 applies, it is easy to show that

$$[B(t)] = \frac{k_f}{(k_f + k_r)}[1 - e^{-(k_f+k_r)t}] \tag{5}$$

if [B(0)] = 0 and [A(0)] = 1 where B refers to any of the modes and k_f and k_r refer to the appropriate forward and reverse rate constants, respectively. Even with the application of the external electric field each forward rate constant is assumed to be much smaller than the corresponding reverse rate constant, and therefore even at equilibrium the fraction of chains that are excited is much less than one. Thus we have neglected the small changes in [A] caused by the buildup of the other modes. Since the forward rate constants are comparatively small, the rise time

$$T_r = 1/(k_f + k_r) \tag{6}$$

is not significantly different than the decay time

$$T_d = 1/k_r \tag{7}$$

Thus in the weak-field limit the rise and decay times are the same, as assumed in eq 2 and 3. As the "concentrations" refer to birefringence amplitudes with specific decay times, the numerical values of $[B_1]$, $[B_2]$, or $[B_3]$ can be increased either by an increase in the fraction of chains with the appropriate mode excited and/or by an increase in the excitation energy of the mode within some of the excited chains. Thus we see that the kinetics scheme of eq 4 will reproduce the ideal behavior of eq 2 and 3 in the low-field limit if the reverse rate constants are not field dependent.

Suppose that we postulate an additional "reaction"

$$[B_2] \underset{k_{4r}}{\overset{k_{4f}}{\rightleftharpoons}} [B_1] \tag{8}$$

which allows excitation energy to be shared between the rotational and first internal modes. We assume the k_{4f} and k_{4r} are large and approximately equal when the external field is applied and essentially zero when there is no field. We also assume that k_{2f} is large compared with k_{1f} under our experimental conditions. With these assumptions about the magnitudes of the various rate constants, the addition of eq 8 allows us to explain some of the nonideal behaviors that we have observed. $[B_1]$ and $[B_2]$ are similar in magnitude during excitation because of the quasi-equilibrium established by eq 8 (this is shown by Figures 7 and 8). $[B_2]$ (the first internal mode) does not grow as fast as it decays (Figure 8) because some of its excitation energy is transferred to B_1 (the rotational mode). This in turn allows $[B_1]$ (the rotational mode) to grow faster than it decays (Figure 7). Since k_{2f} is large compared with k_{1f} and k_{4f} is also large, most of the rotational mode (B_1) is excited by way of the first internal mode (B_2). The time it takes for an appreciable amplitude of B_1 (the first internal mode) to build up accounts for the "lag" seen in the excitation of the rotational mode (B_1) (Figure 7).

What is the significance of this "kinetic" scheme? Equation 8 may represent "segmental orientation" coalescing into "chain rotation", the idea being that the first internal bending mode is excited by the rotation of segments of the overall chain and that the rearrangement of these segments (assumed to be rapid, with rate constants k_{4f} and k_{4r}) can result in a change in configuration equiv-

alent to rotation of the entire chain, i.e. excitation of the rotational mode.

It should be noted that this simple kinetics scheme does not explain the maximum in the excitation time course of the birefringence (Figure 4).

Conclusions

In this work we have measured the amplitudes and decay times of the first three decay modes as a function of pulse duration and strength, showing that the magnitudes of the various decay modes are pulse width and field strength dependent. The field strength dependence is evident even under conditions where a modified form of the Kerr law is obeyed. Our experimental observations are consistent with those of Diekmann et al.,[17] Stellwagen,[18] and our previous work.[1] We have suggested possible pictures of the orientation mechanism of DNA in an electric field. Our hope is that these or similar pictures will give rise to a semiquantitative theory that can successfully explain the relatively complex behavior of flexible DNAs, both in an electric field and after the field is removed.

Acknowledgment. This work was supported through NSF Grant CHE85 11178 and NIH Grant 2 R01 GM 22517 to R.P. and through NIH Grant 2 R01 GM 31674 to D.E. This work was also supported by the NSF MRL program through the Center for Materials Research at Stanford University. R.J.L. was supported by the NIH Medical Scientist Training Program at the Stanford University School of Medicine. D.E. is the recipient of a NIH Research Career Development Award. We appreciate the helpful comments of the reviewers.

References and Notes

(1) Lewis, R. J.; Pecora, R.; Eden, D. *Macromolecules* **1986**, *19*, 134.
(2) Roitman, D. B.; Zimm, B. H. *J. Chem. Phys.* **1984**, *81*, 6333.
(3) Roitman, D. B.; Zimm, B. H. *J. Chem. Phys.* **1984**, *81*, 6348.
(4) Roitman, D. B. *J. Chem. Phys.* **1984**, *81*, 6356.
(5) Zimm, B. H. *J. Chem. Phys.* **1956**, *24*, 269.
(6) Zimm, B. H.; Roe, G. M.; Epstein, L. F. *J. Chem. Phys.* **1956**, *24*, 279.
(7) Lewis, R. J.; Pecora, R. *Macromolecules* **1986**, *19*, 2074.
(8) Nagasaka, K.; Yamakawa, H. *J. Chem. Phys.* **1985**, *83*, 6480.
(9) Lewis, R. J.; Huang, J. H.; Pecora, R. *Macromolecules* **1985**, *18*, 1530.
(10) Provencher, S. W. *Biophys. J.* **1976**, *16*, 27.
(11) Provencher, S. W. *J. Chem. Phys.* **1976**, *64*, 2772.
(12) Provencher, S. W.; Hendrix, J.; De Maeyer, L.; Paulussen, N. *J. Chem. Phys.* **1979**, *69*, 4273.
(13) Provencher, S. W. *Makromol. Chem.* **1979**, *180*, 201.
(14) Provencher, S. W. *CONTIN User's Manual*; European Molecular Biology Laboratory Technical Report EMBL-DA02, Heidelberg, 1980.
(15) Provencher, S. W. *Comput. Phys. Commun.* **1982**, *27*, 213.
(16) Provencher, S. W. *Comput. Phys. Commun.* **1982**, *27*, 229.
(17) Diekmann, S.; Hillen, W.; Morgeneyer, B.; Wells, R. D.; Porschke, D. *Biophys. Chem.* **1982**, *15*, 263.
(18) Stellwagen, N. C. *Biopolymers* **1981**, *20*, 399.
(19) Hagerman, P. J.; Zimm, B. H. *Biopolymers* **1981**, *20*, 1481.
(20) Hagerman, P. J. *Biopolymers* **1981**, *20*, 1503.
(21) Benoit, H. *Ann. Phys. (Paris)* **1951**, *6*, 561.
(22) Mandelkern, M.; Elias, J. G.; Eden, D.; Crothers, D. M. *J. Mol. Biol.* **1981**, *152*, 153.
(23) Gebhard, M. S.; Haleem, M.; Eden, D. *Biophys. J.* **1986**, *49*, 300a.
(24) Porschke, D. *Biophys. Chem.* **1985**, *22*, 237.
(25) Porschke, D. *Annu. Rev. Phys. Chem.* **1985**, *36*, 159.
(26) Elias, J. G.; Eden, D. *Macromolecules* **1981**, *14*, 410.
(27) Hogan, M.; Dattagupta, N.; Crothers, D. M. *Proc. Natl. Acad. Sci. U.S.A.* **1978**, *75*, 195.
(28) Rau, D. C.; Charney, E. *Biophys. Chem.* **1983**, *17*, 35.
(29) Diekmann, S.; Hillen, W.; Jung, M.; Wells, R. D.; Porschke, D. *Biophys. Chem.* **1982**, *15*, 157.
(30) Marion, C.; Perrot, B.; Roux, B.; Bernengo, J. C. *Makromol. Chem.* **1984**, *185*, 1665.
(31) Rau, D. C.; Charney, E. *Biophys. Chem.* **1981**, *14*, 1.
(32) Morita, A.; Watanabe, H. *Macromolecules* **1984**, *17*, 1545.
(33) Meyer, P. I.; Vaughan, W. E. *Biophys. Chem.* **1980**, *12*, 329.
(34) Mandel, M..; Odijk, T. *Annu. Rev. Phys. Chem.* **1984**, *35*, 75.
(35) Balasubramanian, D.; Charney, E. *J. Phys. Chem.* **1981**, *85*, 1943.
(36) Yamaoka, K.; Matsuda, K. *Macromolecules* **1980**, *13*, 1558.
(37) Yoshioka, K. *J. Chem. Phys.* **1983**, *79*, 3482.
(38) Sokerov, S.; Weill, G. *Biophys. Chem.* **1979**, *10*, 161.
(39) Yamaoka, K.; Matsuda, K. *J. Phys. Chem.* **1985**, *89*, 2779.
(40) Tinoco, Jr., I.; Yamaoka, K. *J. Phys. Chem.* **1959**, *63*, 423.
(41) Stellwagen, N. C. *Biophys. Chem.* **1982**, *15*, 311.
(42) Manning, G. S. *Q. Rev. Biophys.* **1978**, *11*, 179.
(43) Manning, G. S. *J. Chem. Phys.* **1969**, *51*, 924.
(44) Manning, G. S. *J. Chem. Phys.* **1969**, *51*, 934.
(45) van Dijk, W.; von der Touw, F.; Mandel, M. *Macromolecules* **1981**, *14*, 792.
(46) Watanabe, H.; Morita, A. *Adv. Chem. Phys.* **1984**, *56*, 255.
(47) Watanabe, H.; Morita, A. *J. Phys. Chem.* **1985**, *89*, 1787.
(48) Morita, A.; Watanabe, H. *J. Phys. Chem.* **1985**, *89*, 5755.
(49) Rau, D. C.; Bloomfield, V. A. *Biopolymers* **1979**, *18*, 2783.
(50) Fixman, M. *J. Chem. Phys.* **1981**, *75*, 4040.
(51) Fixman, M.; Jagannathan, S. *J. Chem. Phys.* **1981**, *75*, 4048.
(52) Pollak, M.; Glick, H. A. *Biopolymers* **1977**, *16*, 1007.
(53) Diekmann, S.; Porschke, D. *Biophys. Chem.* **1982**, *16*, 261.

Tracer Diffusion in Polymeric Mixtures

Walter Hess

Fakultät für Physik, Universität Konstanz, 7750 Konstanz, West Germany, and Max-Planck-Institut für Polymerforschung, 6500 Mainz, West Germany.
Received January 29, 1987

ABSTRACT: In the framework of a microscopic many-body theory the tracer diffusion coefficient is calculated for a system of interacting chains with different lengths. The important argument, which replaces the phenomenological tube concept and allows a concrete solution of the problem, is the translational invariance of the interaction potential for curvilinear displacements of the segments. In a self-consistent way we obtain a reptation transition, where at a critical strength of interaction the lateral motion of the segments freezes in. In the long-chain limit the tracer diffusion coefficient can be decomposed as $D_t = D_{rep} + D_{cr}$, where D_{rep} is the reptation and D_{cr} the constraint release mechanism. Whereas our result for D_{rep} is in agreement with the phenomenological theories, we obtain a much stronger constraint release contribution. For the special case of a monodisperse solution, the constraint release mechanism gives the same contribution to D_t as the reptation mechanism itself.

1. Introduction

Polymeric liquids are distinct from other kinds of liquids, consisting of smaller molecules, because of their spectacular rheological and viscoelastic properties. If a sudden force is exerted on a polymeric liquid, it responds elastically like a rubber. Only if the force acts over a

0024-9297/87/2220-2587$01.50/0